A GENERAL PHASE TRANSITION MODEL FOR VEHICULAR TRAFFIC[*]

S. BLANDIN[†], D. WORK[‡], P. GOATIN[§], B. PICCOLI[¶], AND A. BAYEN[‖]

Abstract. An extension of the Colombo phase transition model is proposed. The congestion phase is described by a two-dimensional zone defined around a standard fundamental diagram. General criteria for building such a set-valued fundamental diagram are enumerated and instantiated on several standard fluxes with different concavity properties. The solution to the Riemann problem in the presence of phase transitions is obtained through the design of a Riemann solver, which enables the construction of the solution of the Cauchy problem using wavefront tracking. The free-flow phase is described using a Newell–Daganzo fundamental diagram, which allows for a more tractable definition of phase transition compared to the original Colombo phase transition model. The accuracy of the numerical solution obtained by a modified Godunov scheme is assessed on benchmark scenarios for the different flux functions constructed.

Key words. partial differential equations, hyperbolic systems of conservation laws, macroscopic highway traffic flow model, phase transition, numerical scheme, Riemann solver

AMS subject classifications. 35L65, 35F25, 65M12, 90B20, 76T99

DOI. 10.1137/090754467

1. Introduction.

First order scalar models of traffic. Hydrodynamic models of traffic go back to the 1950s with the work of Lighthill and Whitham [31] and Richards [38], who built the first model of the evolution of vehicle density on the highway using a first order scalar hyperbolic *partial differential equation* (PDE) referred to as the LWR PDE. Their model relies on the knowledge of an empirically measured *flux function*, also called the *fundamental diagram* in transportation engineering, for which measurements go back to 1935 with the pioneering work of Greenshields [22]. Numerous other flux functions have since been proposed in the hope of capturing effects of congestion more accurately, in particular, Greenberg [21], Underwood [44], Newell [34], Daganzo [10], and Papageorgiou [47]. The existence and uniqueness of an *entropy* solution to the *Cauchy problem* [39] for the class of scalar conservation laws to which the LWR PDE belongs go back to the work of Oleinik [35] and Kruzhkov [27] (see also the seminal article of Glimm [18]), which was extended later to the *initial-boundary value problem* [2] and specifically instantiated for the scalar case with a concave flux function in [29], in particular for traffic in [40]. Numerical solutions of the LWR PDE go back to the seminal *Godunov scheme* [20, 30], which was shown to converge to the entropy solution of the first order hyperbolic PDE (in particular, the LWR

[†]Corresponding author. Systems Engineering, Department of Civil and Environmental Engineering, University of California, Berkeley, CA 94720 (blandin@berkeley.edu).

[‡]Department of Civil and Environmental Engineering, University of Illinois at Urbana-Champaign, 205 North Mathews Ave., Urbana, IL 61801-2352 (dbwork@illinois.edu).

[§]EPI OPALE, INRIA Sophia Antipolis Méditerranée, 06902 Sophia Antipolis Cedex, France (paola.goatin@inria.fr).

[¶]Department of Mathematical Sciences, Rutgers University, Camden, NJ 08102 (piccoli@camden.rutgers.edu).

[‖]Systems Engineering, Department of Civil and Environmental Engineering, University of California, Berkeley, CA 94720 (bayen@berkeley.edu).

PDE). In the transportation engineering community, the Godunov scheme in the case of a triangular flux is known under the name of *cell transmission model* (CTM), which was brought to the field by Daganzo in 1995 [10, 11] (see [28] for the general case) and is one of the most used discrete traffic flow models in the literature today [5, 13, 24, 32, 33, 36, 46].

Set-valued fundamental diagrams. The assumption of a Greenshields fundamental diagram or a triangular *fundamental diagram*, which significantly simplifies the analysis of the model algebraically, led to the aforementioned theoretical developments. Yet, experimental data clearly indicate that while the free-flow part of a fundamental diagram can be approximated fairly accurately by a straight line, the congested regime is set-valued and can hardly be characterized by a single curve [45]. An approach for modeling the set-valuedness of the congested part of the fundamental diagram consists of using a second equation coupled with the mass conservation equation (i.e., the LWR PDE model). Such models go back to Payne [37] and Whitham [48] and generated significant research efforts, which led, however, to models with inherent weaknesses that were later pointed out by Del Castillo [15] and Daganzo [12]. These weaknesses were ultimately addressed in several responses [1, 36, 49], leading to sustained research in this field.

Motivation for a new model. Despite the existing research, modeling issues remain in most 2×2 models of traffic available today. For instance, the *Aw–Rascle* model [1] can introduce vanishing velocities below jam density, which is not a classical assumption in traffic theory [17]. In agreement with the remarks from Kerner [25, 26] affirming that traffic flow presents three different behaviors, *free-flow*, *wide moving jams*, and *synchronized flow*, Colombo proposed a 2×2 phase transition model [7, 8] which considers *congestion* and *free-flow* in traffic as two different phases, governed by distinct evolutionary laws (see also [19] for a phase transition version of the Aw–Rascle model). The well-posedness of this model was proved in [9] using *wavefront tracking* techniques [4, 23]. In the phase transition model, the evolution of the parameters is governed by two distinct dynamics; in *free-flow*, the Colombo phase transition model is a classical first order model (LWR PDE), whereas in *congestion* a similar equation governs the evolution of an additional state variable, the *linearized momentum q*. The motivation for an extension of the 2×2 phase transition model comes from the following items, which are addressed by the class of models presented in this article.

(i) *Phases gap.* The phase transition model introduced by Colombo in [7] uses a Greenshields flux function to describe *free-flow*, which despite its simple analytical expression yields a fundamental diagram which is not connected and thus a complex definition of the solution to the Riemann problem between two different phases. We solve this problem by introducing a Newell–Daganzo flux function for *free-flow*, which creates a nonempty intersection between the congested phase and the *free-flow* phase, called the *metastable phase*. It alleviates the inconvenience of having to use a shock-like phase transition in many cases of the Riemann problem between two different phases.

(ii) *Definition of a general class of set-valued fundamental diagrams.* The work achieved in [8] enables the definition of a set-valued fundamental diagram for the expression of the velocity function introduced. However, experimental data show that several types of fundamental diagram exist, with different congested domain shapes. In this article we provide a method for building an arbitrary set-valued fundamental diagram, which in a special case corresponds to the fundamental diagram introduced in [7]. This enables one to define a custom-made set-valued fundamental diagram.

Organization of the article. The rest of the article is organized as follows. Section 2 presents the fundamental features of the Colombo phase transition model [8], which serves as the basis for the present work. In section 3, we introduce the modifications to the Colombo phase transition model, and introduce the notion of *standard state* which provides the basis for the construction of a class of 2×2 traffic models. We also assess general conditions which enable us to extend the results obtained for the original Colombo phase transition model to these new models. Finally, section 3 presents a modified *Godunov scheme* which can be used to solve the equations numerically. The following two sections instantiate the constructed class of models for two specific flux functions, which are the Newell–Daganzo (affine) flux function (section 4) and the Greenshields (parabolic concave) flux function (section 5). Each of these sections includes a discussion of the choice of parameters needed for each of the models, the solution to the Riemann problem, a description of the specific properties of the model, and a validation of the numerical results using a benchmark test. Finally, section 6 presents some concluding remarks.

2. The Colombo phase transition model. The original Colombo phase transition model [7, 8] is a set of two coupled PDEs valid in a *free-flow* regime and a *congested* regime, respectively:

(2.1)
$$\begin{cases} \partial_t \rho + \partial_x(\rho\, v_f(\rho)) = 0 & \text{in free-flow } (\Omega_f), \\ \begin{cases} \partial_t \rho + \partial_x(\rho\, v_c(\rho, q)) = 0 \\ \partial_t q + \partial_x((q - q^*)\, v_c(\rho, q)) = 0 \end{cases} & \text{in congestion } (\Omega_c), \end{cases}$$

where the state variables ρ and q denote, respectively, the density and the *linearized momentum* [8]. Ω_f and Ω_c are the respective domains of validity of the free-flow and congested equations of the model and are defined below. The term q^* is a characteristic parameter of the road under consideration. An empirical relation expresses the velocity v as a function of density in free-flow, $v := v_f(\rho)$, and as a function of density and linearized momentum in congestion, $v := v_c(\rho, q)$. Following the usual choices for traffic applications [16], the following functions are used:

$$v_f(\rho) = \left(1 - \frac{\rho}{R}\right) V \quad \text{and} \quad v_c(\rho, q) = \left(1 - \frac{\rho}{R}\right) \frac{q}{\rho},$$

where R is the maximal density or *jam density* and V is the maximal *free-flow speed*. The relation for free-flow is the *Greenshields* model [22] mentioned earlier, while the second relation has been introduced in [7]. Since Ω_c has to be an invariant domain [39] for the congested dynamics from system (2.1), and according to the definition of v, the free-flow and congested domains are defined as

$$\begin{cases} \Omega_f = \left\{ (\rho, q) \in [0, R] \times [0, +\infty[\; , v_f(\rho) \geq V_{f-}\; , \; q = \rho V \right\}, \\ \Omega_c = \left\{ (\rho, q) \in [0, R] \times [0, +\infty[\; , v_c(\rho, q) \leq V_{c+}\; , \; \frac{Q^- - q^*}{R} \leq \frac{q - q^*}{\rho} \leq \frac{Q^+ - q^*}{R} \right\}, \end{cases}$$

where V_{f-} is the minimal velocity in free-flow and V_{c+} is the maximal velocity in congestion such that $V_{c+} < V_{f-} < V$. R is the maximal density and Q^- and Q^+ are, respectively, the minimal and maximal values for q. The fundamental diagrams in (ρ, q) coordinates and in $(\rho, \rho v)$ coordinates are presented in Figure 2.1.

Remark 2.1. The congested part of system (2.1) is strictly hyperbolic if and only if the two eigenvalues of its Jacobian are real and distinct for all states $(\rho, q) \in \Omega_c$.
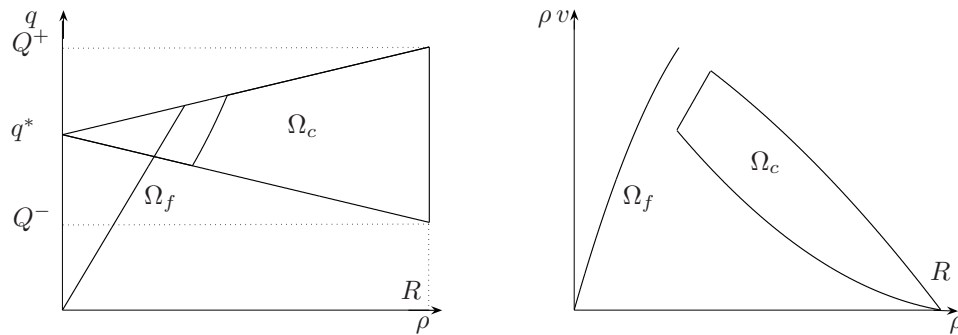
FIG. 2.1. *Colombo phase transition model. Left: Fundamental diagram in state space coordinates* (ρ, q). *Right: Fundamental diagram in density flux coordinates* $(\rho, \rho\, v)$.

Remark 2.2. The 1-Lax curves are straight lines going through $(0, q^*)$ in (ρ, q) coordinates, which means that along these curves shocks and rarefactions exist and coincide [41]. One must note that the 1-Lax field is not *genuinely nonlinear* (GNL). Indeed the 1-Lax curves are *linearly degenerate* (LD) for $q = q^*$ and GNL otherwise, with rarefaction waves propagating in different directions relative to the eigenvectors depending on the sign of $q - q^*$. The 2-Lax curves, which are straight lines going through the origin in $(\rho, \rho\, v)$ coordinates, are always LD.

3. Extension of the Colombo phase transition model. The approach, developed by Colombo, provides a fundamental diagram which is thick in congestion (Figure 2.1) and thus can model clouds of points observed experimentally (Figure 3.1). We propose extending this approach by considering the second equation in congestion as modeling a perturbation [49, 50]. The *standard state* (Definition 3.1) would be the usual one-dimensional fundamental diagram, with dynamics described by the conservation of mass. Perturbations can move the system off standard state, leading the diagram to span a two-dimensional area in congestion. A single-valued map is able to describe the free-flow mode, which is therefore completely described by the free-flow standard state.

DEFINITION 3.1. *We denote by* standard state *the set of states described by a one-dimensional fundamental diagram and the classical LWR PDE. In the following we refer to the standard velocity and standard flux as the velocity and flux, respectively, at the standard state.*

In this section we present analytical requirements on the velocity function in congestion, which, given the work done in [8], enable us to construct a 2×2 phase transition model. These models provide support for a physically correct, mathematically well-posed initial-boundary value problem which can model traffic phenomena where the density and the flow are independent quantities in congestion, allowing for multiple values of the flow for a given value of the density. Our framework allows one to define the two-dimensional zone span by the congestion phase according to the reality of the local traffic nature, which is not always possible with the original Colombo phase transition model.

3.1. Analysis of the standard state. We consider the density variable ρ to belong to the interval $[0, R]$, where R is the maximal density. Given the *critical*
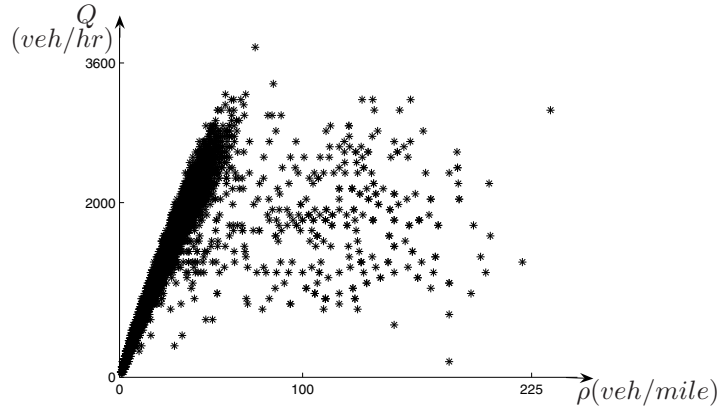
FIG. 3.1. *Fundamental diagram in density flux coordinates from a street in Rome. In congestion (high densities) the flux is multivalued. Count C and velocity v were recorded every minute during one week. Flux Q was computed from the count. Density ρ was computed from flux and velocity according to the expression $Q = \rho\, v$ (see [3] for an extensive analysis of this dataset).*

density[1] σ in $(0, R]$, we define the standard velocity $v^s(\cdot)$ on $[0, R]$ by

$$v^s(\rho) := \begin{cases} V & \text{for } \rho \in [0, \sigma], \\ v_c^s(\rho) & \text{for } \rho \in [\sigma, R], \end{cases}$$

where V is the free-flow speed and $v_c^s(\cdot)$ is in $C^\infty((\sigma_-, R), \mathbb{R}^+)$. It is important to note that $v_c^s(\cdot)$ is a function of ρ only, as is the case for the classical fundamental diagram. The standard flux $Q^s(\cdot)$ is thus defined on $[0, R]$ by

$$Q^s(\rho) := \rho\, v^s(\rho) = \begin{cases} Q_f(\rho) := \rho\, V & \text{for } \rho \in [0, \sigma], \\ Q_c^s(\rho) := \rho\, v_c^s(\rho) & \text{for } \rho \in [\sigma, R]. \end{cases}$$

In agreement with traffic flow features, the congested standard flux $Q_c^s(\rho)$ must satisfy the following requirements (which are consistent with those given in [14]).

(i) *Flux vanishes at the maximal density*: $Q_c^s(R) = 0$.
This condition encodes the physical situation in which the jam density has been reached. The corresponding velocity and flux of vehicles on the highway is zero.

(ii) *Flux is a decreasing function of density in congestion*: $dQ_c^s(\rho)/d\rho \leq 0$.
This is required as a defining property of congestion. It implies that $dv_c^s(\rho)/d\rho \leq 0$.

(iii) *Continuity of the flux at the critical density*: $Q_c^s(\sigma) = Q_f(\sigma)$.
Even if some models account for a discontinuous flux at capacity (the *capacity drop* phenomenon [26]), we assume, following most of the transportation community, that the flux at the standard state is a continuous function of density.

(iv) *Concavity of the flux in congestion*: $Q_c^s(\cdot)$.
The flux function at the standard state $Q_c^s(\cdot)$ must be concave on $[\sigma, \sigma_i]$ and convex on $[\sigma_i, R]$, where σ_i is in (σ, R). Given the experimental datasets obtained for congestion (Figure 3.1), it is not clear in practice if the standard flux is concave or convex in congestion. The assumption made here is motivated by Remark 3.14.

---

[1]Density for which the flux is maximal at the standard state. At this density the system switches between free-flow and congestion.

Remark 3.2. In this article we instantiate the general model proposed on the most common standard flux functions (i.e., linear or concave) but the framework developed here applies to flux functions with changing concavity such as the Li flux function [42], although it yields a significantly more complex analysis.

3.2. Analysis of the perturbation.

3.2.1. Model outline. In this section we introduce a perturbation q to the standard velocity in congestion.

DEFINITION 3.3. *The perturbed velocity function $v_c(\cdot, \cdot)$ is defined on Ω_c by*

$$v_c(\rho, q) = v_c^s(\rho)\,(1 + q), \tag{3.1}$$

where $v_c^s(\cdot) \in C^\infty((\sigma_-, R), \mathbb{R}^+)$ is the congested standard velocity function.

The standard state corresponds to $q = 0$, and the evolution of (ρ, q) is described similarly to the classical Colombo phase transition model [8] by

$$\begin{cases} \partial_t \rho + \partial_x(\rho\,v) = 0 & \text{in free-flow,} \\ \begin{cases} \partial_t \rho + \partial_x(\rho\,v) = 0 \\ \partial_t q + \partial_x(q\,v) = 0 \end{cases} & \text{in congestion,} \end{cases} \tag{3.2}$$

with the following expression of the velocity:

$$v = \begin{cases} v_f(\rho) := V & \text{in free-flow,} \\ v_c(\rho, q) & \text{in congestion.} \end{cases} \tag{3.3}$$

The perturbed velocity function defines the velocity in congestion, whereas a Newell–Daganzo function describes the velocity in free-flow. The analytical expression of the free-flow and congested domains as defined in (3.4) is motivated by the analysis conducted in Table 3.1 and the necessity for these domains to be invariants [39] for the dynamics (3.2) in order to have a well-defined Riemann solver [43]:

$$\begin{cases} \Omega_f = \{(\rho, q) \mid (\rho, q) \in [0, R] \times [0, +\infty[\ ,\ v_c(\rho, q) = V\ ,\ 0 \le \rho \le \sigma_+\}, \\ \Omega_c = \left\{(\rho, q) \mid (\rho, q) \in [0, R] \times [0, +\infty[\ ,\ v_c(\rho, q) < V\ ,\ \frac{q_-}{R} \le \frac{q}{\rho} \le \frac{q_+}{R}\right\}. \end{cases} \tag{3.4}$$

$\sigma_\pm$ is defined by $v_c(\sigma_\pm, \sigma_\pm q_\pm/R) = V$, and we assume that $V > 0$ and $q_- \le 0 \le q_+$. A definition of the complete set of parameters can be found in section 3.3 (see also Figure 3.2 for an illustration in the Newell–Daganzo case).

DEFINITION 3.4. *The set $\{(\rho, q) \mid v_c(\rho, q) = V, \sigma_- \le \rho \le \sigma_+\}$ defines the metastable phase. This phase defines transition states between the congestion phase and the free-flow phase.*

Remark 3.5. The left boundary of the congested domain is a convex curve in (ρ, q) coordinates (shown in Figure 2.1 for the Colombo phase transition model and in Figure 3.2 for the new model derived). Thus Ω_c is not convex in (ρ, q) coordinates.

The analysis of the congestion phase of the model (3.2) is outlined in Table 3.1.

3.2.2. Physical and mathematical considerations. Physical interpretation and mathematical conditions translate into the following conditions.

CONDITION 3.6 (*positivity of speed*). *In order to maintain positivity of $v_c(\cdot, \cdot)$ on the congested domain, one must have*

$$\forall\, q \in [q_-, q_+], \quad 1 + q > 0, \tag{3.5}$$

TABLE 3.1
Congestion phase: algebraic properties of the general phase transition model.

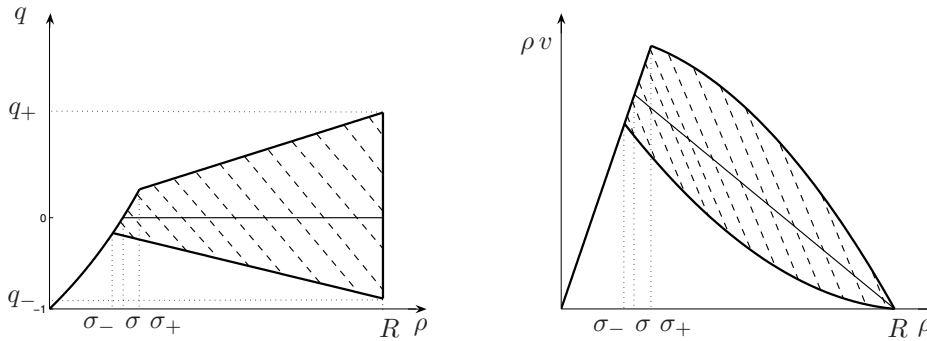| Eigenvalues	$\lambda_1(\rho, q) = \rho\,(1+q)\partial_\rho v_c^s(\rho) + v_c^s(\rho)\,(1+2\,q)$	$\lambda_2(\rho, q) = v_c^s(\rho)\,(1+q)$
Eigenvectors	$r_1 = \begin{pmatrix} \rho \\ q \end{pmatrix}$	$r_2 = \begin{pmatrix} v_c^s(\rho) \\ -(1+q)\,\partial_\rho v_c^s(\rho) \end{pmatrix}$
Nature of the Lax curves	$\nabla\lambda_1.r_1 = \rho^2\,(1+q)\partial_{\rho\rho}^2 v_c^s(\rho) + 2\,\rho\,(1+2\,q)\,\partial_\rho v_c^s(\rho) + 2\,q\,v_c^s(\rho)$	$\nabla\lambda_2.r_2 = 0$
Riemann-invariants	q/ρ	$v_c^s(\rho)\,(1+q)$

FIG. 3.2. *Newell–Daganzo standard flux function. Left: Fundamental diagram in state space coordinates. Right: Fundamental diagram in flux-density coordinates. The standard state is the usual triangular diagram. The congestion phase is two-dimensional (striped domain).*

which is satisfied if and only if $q_- > -1$.

CONDITION 3.7 (*strict hyperbolicity of the congested system*). *In order for the congested part of* (3.2) *to be strictly hyperbolic, one must have*

$$\forall\,(\rho, q) \in \Omega_c, \quad \lambda_1(\rho, q), \lambda_2(\rho, q) \in \mathbb{R} \quad and \quad \lambda_1(\rho, q) \neq \lambda_2(\rho, q).$$

Given the expression of the eigenvalues outlined in Table 3.1, *and modulo a rearrangement, this yields*

$$(3.6) \qquad \forall\,(\rho, q) \in \Omega_c, \quad \rho\,\partial_\rho v_c^s(\rho) + q\,(v_c^s(\rho) + \rho\,\partial_\rho v_c^s(\rho)) \neq 0.$$

Since $v_c^s(\cdot)$ is positive and $\rho\,v_c^s(\cdot)$ is a decreasing function of ρ, this can always be satisfied for small enough values of q, and when instantiated for specific expressions of $v_c^s(\cdot)$, will result in a bound on the perturbation q.

CONDITION 3.8 (*shape of Lax curves*). *For modeling consistency, we require the 1-Lax curves to be LD or to have no more than one inflexion point (σ_i, q_i). In the latter case they should be concave for $\rho \leq \sigma_i$ and convex for $\rho \geq \sigma_i$. Since $\nabla\lambda_1.r_1$ is the second derivative of the 1-Lax curve with respect to ρ, this condition can be enforced, for any (ρ, q) in the congested domain, by checking the sign of the expression*

$$(3.7) \qquad \nabla\lambda_1.r_1 = \rho\,(2\,\partial_\rho v_c^s(\rho) + \rho\,\partial_{\rho\rho}^2 v_c^s(\rho)) + q\,(2\,v_c^s + 4\,\rho\,\partial_\rho v_c^s(\rho) + \rho^2\,\partial_{\rho\rho}^2 v_c^s(\rho)),$$

which has the sign of the first term for q small enough. So if $2\,\partial_\rho v_c^s(\rho) + \rho\,\partial_{\rho\rho}^2 v_c^s(\rho) > 0$, the rarefaction waves go right in the (ρ, q) or $(\rho, \rho v)$ plane. When $v_c^s(\cdot)$ is such that $2\,\partial_\rho v_c^s(\rho) + \rho\,\partial_{\rho\rho}^2 v_c^s(\rho) = 0$, the heading of rarefaction waves changes with the sign of

q (such is also the case for the original phase transition model), and in this case the 1-curves are LD for q = 0.

This condition consists of ensuring that expression (3.7) *is either identically zero (LD curve), or has no more than one zero and is an increasing function of the density.*

Remark 3.9. One may note that Condition 3.7 on the strict hyperbolicity of the system is satisfied whenever Condition 3.6 on the positivity of speed is satisfied. Indeed, (3.6) can be rewritten as $\forall (\rho, q) \in \Omega_c$, $\rho \, \partial_\rho v_c^s(\rho) + q \partial_\rho Q_c^s(\rho) \neq 0$, which since the first term is negative, is equivalent to $\forall (\rho, q) \in \Omega_c$, $\rho \, \partial_\rho v_c^s(\rho) + q \partial_\rho Q_c^s(\rho) < 0$. For nonzero values of $\partial_\rho Q_c^s(\rho)$, it yields $q > -\rho \, \partial_\rho v_c^s(\rho)/\partial_\rho Q_c^s(\rho) = -1 + v_c^s(\rho)/\partial_\rho Q_c^s(\rho)$, which is always satisfied when $q_- > -1$, because the second term of the right-hand side is negative.

Remark 3.10. In this model, traffic is anisotropic in the sense that no wave travels faster than vehicles $(\lambda_1(\rho, q) < \lambda_2(\rho, q) = v_c(\rho, q))$. The speed of vehicles is always positive, and they stop only at maximal density.

3.3. Definition of parameters. The parameters of the proposed model are the

  (i) free-flow speed V,
  (ii) maximal density R,
  (iii) critical density σ at standard state,
  (iv) critical density for the lower bound of the diagram σ_-,
  (v) critical density for the upper bound of the diagram σ_+.

These parameters can be identified from experimental data and enable the definition of the parameters q_- and q_+. Figure 3.2 graphically summarizes the definition of the parameters chosen. One must note that the constraints on q_-, q_+ detailed in (3.5), (3.6), and (3.7) translate into constraints on σ_-, σ_+, which cannot be freely chosen.

3.4. Cauchy problem. In this section we define a solution to the Cauchy problem for the system (3.2). Following [8], we use a definition derived from [4].

DEFINITION 3.11. *Given T in $\mathbb{R}_+$ and u_0 in $L^1(\mathbb{R}; \Omega_f \cup \Omega_c) \cap BV(\mathbb{R}; \Omega_f \cup \Omega_c)$, an admissible solution to the corresponding Cauchy problem for* (3.2) *is a function $u(\cdot, \cdot)$ in $L^1([0, T] \times \mathbb{R}; \Omega_f \cup \Omega_c) \cap BV([0, T] \times \mathbb{R}; \Omega_f \cup \Omega_c)$ such that the following hold.*

  (i) *For all t in $[0, T]$, $t \mapsto u(t, .)$ is Lipshitz continuous with respect to the L^1 norm.*

  (ii) *For all functions φ in $C_c^1([0, T] \times \mathbb{R} \mapsto \mathbb{R})$ with compact support contained in $u^{-1}(\Omega_f)$,*

$$\int_0^T \int_{\mathbb{R}} (u(t, x) \, \partial_t \varphi(t, x) + Q_f(u(t, x)) \partial_x \varphi(t, x)) \, dx dt + \int_{\mathbb{R}} u_0(x) \, \varphi(0, x) dx = 0.$$

  (iii) *For all functions φ in $C_c^1([0, T] \times \mathbb{R} \mapsto \mathbb{R}^2)$ with compact support contained in $u^{-1}(\Omega_c)$,*

$$\int_0^T \int_{\mathbb{R}} (u(t, x) \, \partial_t \varphi(t, x) + Q_c(u(t, x)) \partial_x \varphi(t, x)) \, dx dt + \int_{\mathbb{R}} u_0(x) \, \varphi(0, x) dx = 0.$$

  (iv) *The set of points (t, x) for which there is a change of phase is the union of a finite number of Lipschitz curves $p_i : [0, T) \mapsto \mathbb{R}$ such that if $\exists i \neq j$ and $\exists \tau \in [0, T]$ such that $p_i(\tau) = p_j(\tau)$, then for all $t \in [\tau, T]$ we have $p_i(t) = p_j(t)$.*

(v) *For all points (t, x) where there is a change of phase, let $\Lambda = \dot{p}_i(t^+)$, and introducing the left and right flow at (t, x),*

$$F^l = \begin{cases} \rho(t, x^-) \, V & \text{if } \rho(t, x^-) \in \Omega_f, \\ \rho(t, x^-) \, v_c(\rho(t, x^-), q(t, x^-)) & \text{if } \rho(t, x^-) \in \Omega_c, \end{cases}$$

$$F^r = \begin{cases} \rho(t, x^+) \, V & \text{if } \rho(t, x^+) \in \Omega_f, \\ \rho(t, x^+) \, v_c(\rho(t, x^+), q(t, x^+)) & \text{if } \rho(t, x^+) \in \Omega_c, \end{cases}$$

the following relation must be satisfied:

$$(3.8) \qquad \Lambda \cdot (\rho(t, x_+) - \rho(t, x_-)) = F_r - F_l.$$

Remark 3.12. This definition matches the standard Lax entropy solution for an initial condition with values in Ω_f or Ω_c. Equation (3.8) is a Rankine–Hugoniot relation needed to ensure mass conservation at the phase transition.

THEOREM 3.13. *Let Ω_f and Ω_c be defined by* (3.4), *and let $v_c(\cdot, \cdot)$ be defined by* (3.1). *If Condition* 3.7 *is satisfied, then for all $u_0 \in L^1(\mathbb{R}; \Omega_f \cup \Omega_c) \cap BV(\mathbb{R}; \Omega_f \cup \Omega_c)$, the corresponding Cauchy problem for* (3.2) *has an admissible solution (see Definition* 3.11*) $u(\cdot, \cdot)$ such that $u(t, \cdot) \in BV(\mathbb{R}; \Omega_f \cup \Omega_c)$ for all $t \in [0, T]$.*

Proof. A solution is constructed through a standard wavefront tracking procedure by iteratively gluing together the solution to Riemann problems corresponding to piecewise constant approximations of the solution. Measuring total variation along the trajectories of these solutions allows us to conclude on the convergence of the sequence of successive approximations. The interested reader is referred to [4] for more details on wavefront tracking techniques and to [8, 9] for more insights on proofs of existence for systems of conservation laws with phase transition. $\quad\square$

3.5. Model properties. The main differences between the original Colombo model [8] and the class of models introduced in this article result from the following design choices.

Choice of $q^* = 0$. This is a change of variable which has several consequences. Related computations become more readable. The congested standard state is $q = 0$. According to (3.1), the meaning of the perturbation q is also more intuitive. Positive values of q correspond to elements of flow moving at a greater speed than the standard speed for this density, and negative values of q correspond to slower elements of flow. In the traffic context, this can be understood as groups of drivers being characterized by their degree of agressivity, q, which leads them to drive faster or slower than the standard driver.

Newell–Daganzo flux function in free-flow. This allows the free-flow and congested domain of the fundamental diagram proposed in the present work to be connected and to define a metastable phase, as illustrated in Figure 3.3. This yields a well-posed Riemann problem which can be solved in a simple way (see Remark 2 of [8]). Moreover, the derived models need fewer parameters and thus are easier to calibrate. Finally, it is consistent with the fact that a gap between phases is not observed in experimental data; see Figure 3.1.

The expression of the function v_c is not fully specified. This allows us to customize the model depending on the features observed in practice. As explained in Remark 3.14 below, the concavity of the 1-Lax curves is related to driving behavior. In the class of models we introduce, since $v_c(\cdot, \cdot)$ is not fully specified, in the limit of
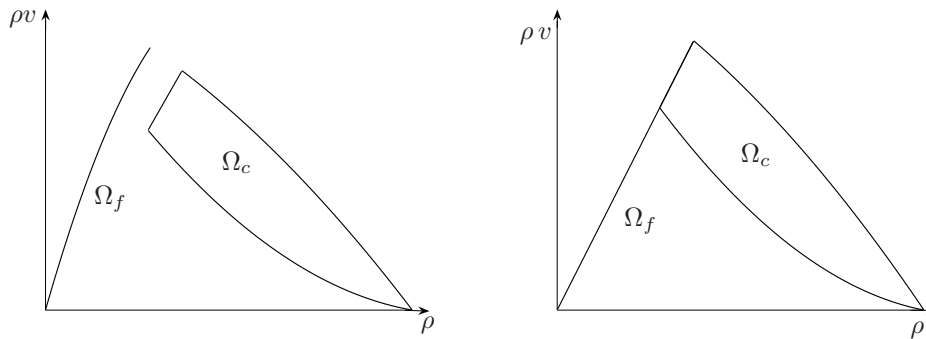
FIG. 3.3. *Different free-flow phases. Left: Fundamental diagram from the original Colombo phase transition model. Right: Fundamental diagram of the model derived in the present article in the particular case of a Newell–Daganzo standard state flux in the congestion phase.*

Conditions 3.6, 3.7, and 3.8, it is possible to define the perturbed phase transition model, which corresponds to the observed driver agressivity.

Remark 3.14. A physical interpretation can be given to the concavity of the flux function. In congestion, when the density increases toward the maximal density, the velocity decreases toward zero. This yields a decreasing slope of the flux function in congestion. The way in which a driver's velocity decreases impacts the concavity of the flux, as per the expression of the second derivative of the standard flux function, $d^2 Q_c^s(\rho)/d\rho^2 = \rho \, d^2 v_c^s(\rho)/d\rho^2 + 2 \, dv_c^s(\rho)/d\rho$.

(i) If for a given density increase, the drivers reduce their speeds more at high densities than at low densities (modeling aggressive drivers who wait until high density to reduce speed), then the velocity function is concave and the flux function is concave.

(ii) If the drivers reduce their speeds less at high densities than at low densities (modeling careful drivers who anticipate and reduce their speed early), then the velocity function is convex, and the flux function may be convex.

(iii) An affine flux is given by a velocity function which satisfies $\rho \, d^2 v_c^s(\rho)/d\rho^2 + 2 \, dv_c^s(\rho)/d\rho = 0$.

3.6. Numerics. Because of the nonconvexity of the domain $\Omega_f \cup \Omega_c$ (illustrated in Figure 3.2), using the classical Godunov scheme [30] is not feasible due to the projection step of the scheme. We propose using a modified version of the scheme (see [6]) which mimics the two steps of the classical Godunov scheme and adds a final sampling step.

(i) The Riemann problems are solved on a regular time space mesh. When two space-consecutive cells do not belong to the same phase, the position of the phase transition at the next time step is computed.

(ii) The solutions are averaged on the domains defined by the position of the phase transitions arising from Riemann problems at neighboring cells (Figure 3.4).

(iii) A sampling method is used to determine the value of the solution in each cell of the regular mesh.

This process addresses the issues of the classical Godunov scheme with nonconvex domains. Numerical results have shown that it gives accurate results on benchmark tests (we refer the reader to [6] for more details on the test cases used).

Let us denote by Δt the time discretization and by Δx the space discretization satisfying the *Courant–Friedrichs–Lewy* condition [30]. We call $x_j = j \, \Delta x$ for $j \in \mathbb{Z}$
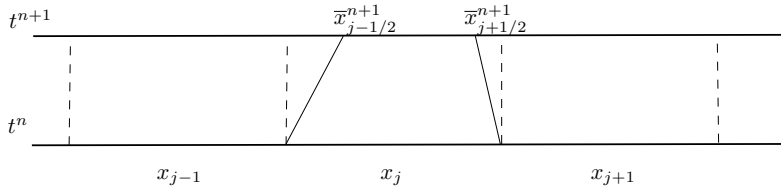
FIG. 3.4. *Phase transitions enter cell C_j^n from both sides.*

and $t_n = n \Delta t$ for $n \in \mathbb{N}$. We call $x_{j-1/2} = x_j - \Delta x/2$ and we define a cell $C_j^n = \{t_n\} \times [x_{j-1/2}, x_{j+1/2}[$, which has length Δx. We call u_j^n the value of $u := (\rho, q)$ at (t_n, x_j), and, by extension, in C_j^n. The speed of the phase transition between each pair of cells (C_j^n, C_{j+1}^n) is denoted $\nu_{j+1/2}^n$ ($\nu_{j+1/2}^n$ equals zero if u_j^n and u_{j+1}^n belongs to the same phase). If we call $\overline{x}_{j-1/2}^{n+1} = x_{j-1/2} + \nu_{j-1/2}^n \Delta t$, we can define cell $\overline{C}_j^{n+1}$ as $\overline{C}_j^{n+1} = \{t_{n+1}\} \times [\overline{x}_{j-1/2}^{n+1}, \overline{x}_{j+1/2}^{n+1}[$, which has length $\Delta \overline{x}_j^n = \overline{x}_{j+1/2}^{n+1} - \overline{x}_{j-1/2}^{n+1}$, as shown in Figure 3.4. The solution to the Riemann problem between cells C_j^n is averaged on cells $\overline{C}_j^{n+1}$, which by construction enclose states which are either free-flowing or congested, according to the modified Godunov scheme.

We define the following:

(i) $u_R(\nu_{j-1/2}^{n,+}, u_{j-1}^n, u_j^n)$ is the solution to the Riemann problem between u_{j-1}^n and u_j^n, at $\frac{x - x_{j-1/2}}{t - t_n} = \nu_{j-1/2}^n$, taken at the right of the phase transition.

(ii) $g(\nu_{j+1/2}^{n,-}, u_j^n, u_{j+1}^n) := f(u_R(\nu_{j+1/2}^{n,-}, u_j^n, u_{j+1}^n))$ with $f(\rho, q) = (\rho v, q v)$ and the definition of v from (3.3), as the numerical flux between cells C_j^n and C_{j+1}^n, at $\frac{x - x_{j+1/2}}{t - t_n} = \nu_{j+1/2}^n$, taken at the left of the phase transition.

The averaging step of the modified Godunov scheme reads as

$$\Delta \overline{x}_j^n \, \overline{u}_j^{n+1} = \Delta x \, u_j^n - \Delta t \left(g\left(\nu_{j+1/2}^{n,-}, u_j^n, u_{j+1}^n\right) - \nu_{j+1/2}^n \, u_R\left(\nu_{j+1/2}^{n,-}, u_j^n, u_{j+1}^n\right) \right)$$
$$+ \Delta t \left(g\left(\nu_{j-1/2}^{n,+}, u_{j-1}^n, u_j^n\right) - \nu_{j-1/2}^n \, u_R\left(\nu_{j-1/2}^{n,+}, u_{j-1}^n, u_j^n\right) \right).$$

One can notice that when there is no phase transition, $\nu_{j-1/2}^n = \nu_{j+1/2}^n = 0$, $\Delta x = \Delta \overline{x}_j^n$, and we obtain the classical Godunov scheme. The last step is the sampling phase to define the solutions on the cells C_j^{n+1}. Following [6], for cell C_j^{n+1} we randomly pick a value between $\overline{u}_{j-1}^{n+1}$, $\overline{u}_j^{n+1}$, and $\overline{u}_{j+1}^{n+1}$ according to their rate of presence in cell C_j^{n+1}. This is done using the Van der Corput sequence $(a_n)_{n \in \mathbb{N}}$ (3.9), which is a low-discrepancy sequence in the interval $[0, 1]$:

$$(3.9) \quad u_j^{n+1} = \begin{cases} \overline{u}_{j-1}^{n+1} & \text{if } a_n \in \,]0, \max(\frac{\Delta t}{\Delta \overline{x}_j^n} \nu_{j-1/2}^n, 0)], \\ \overline{u}_j^{n+1} & \text{if } a_n \in \,]\max(\frac{\Delta t}{\Delta \overline{x}_j^n} \nu_{j-1/2}^n, 0), 1 + \min(\frac{\Delta t}{\Delta \overline{x}_j^n} \nu_{j+1/2}^n, 0)[, \\ \overline{u}_{j+1}^{n+1} & \text{if } a_n \in [1 + \min(\frac{\Delta t}{\Delta \overline{x}_j^n} \nu_{j+1/2}^n, 0), 1[. \end{cases}$$

Remark 3.15. In the general case the congested domain Ω_c is not convex in (ρ, q) coordinates due to the convexity of the metastable border of the domain as illustrated in Figure 3.2. It is therefore necessary to add a projection step as a fourth step to the modified Godunov scheme. The projection (ρ_p, q_p) of state (ρ, q) is defined as the

solution in the metastable phase of the system

$$
\begin{cases}
\frac{q_p}{\rho_p} = \frac{q}{\rho}, \\
v_c(\rho_p, q_p) = V.
\end{cases}
$$

The error metric chosen to assess the numerical accuracy of the scheme is the $C^0(\mathbb{R}, L^1(\mathbb{R}, \mathbb{R}^2))$ relative error between the computed solution and the analytical solution. We call u and u_c the exact and computed solutions respectively. For the computational domain $[x_0, x_1]$, the error at T is computed as follows:

$$
E(T) = \frac{\sup_{t \in [0,T]} \int_{x_0}^{x_1} \|u(t,x) - u_c(t,x)\|_1 dx}{\sup_{t \in [0,T]} \int_{x_0}^{x_1} \|u(t,x)\|_1 dx}.
$$

4. The Newell–Daganzo phase transition model. In this section, we use a Newell–Daganzo velocity function for congestion, i.e., a velocity function for which the flux is affine with respect to the density. We instantiate the corresponding phase transition model for this flux function and derive a corresponding Riemann solver, which we implement and test on a benchmark case.

4.1. Analysis. We propose using the standard velocity function

$$
v_c^s(\rho) = \frac{V\sigma}{R-\sigma} \left(\frac{R}{\rho} - 1 \right),
$$

which is clearly the unique function yielding an affine flux and satisfying the requirements from section 3.1 on the vanishing point, trend, continuity, and concavity property of the standard flux.

For a perturbed state, the velocity function reads as

$$
(4.1) \qquad
\begin{cases}
v_f(\rho) = V & \text{for } (\rho, q) \in \Omega_f, \\
v_c(\rho, q) = \frac{V\sigma}{R-\sigma} \left(\frac{R}{\rho} - 1 \right)(1 + q) & \text{for } (\rho, q) \in \Omega_c,
\end{cases}
$$

where Ω_f and Ω_c are defined by (3.4). The corresponding fundamental diagram is shown in Figure 3.2. The standard flux is affine with the density, but the 1-Lax curves outside the standard state are either convex or concave in $(\rho, \rho v)$ coordinates, depending on the sign of the perturbation.

Remark 4.1. Note that the expression of the velocity in Figure 3.2 is given by (4.1) and depends on the phase and is therefore set-valued for $\rho > \sigma_-$, which is the lowest density value at which congestion can arise.

The conditions from section 3.2 that are necessary to have positive speed and strict hyperbolicity of the congested part of the system (3.2) reduce to

$$
q_- > -1.
$$

4.2. Solution to the Riemann problem. Following [8], we construct the solution to the Riemann problem for the system (3.2) with the velocity function defined by (4.1) and the initial datum

$$
(\rho, q)(0, x) =
\begin{cases}
(\rho_l, q_l) & \text{if } x < 0, \\
(\rho_r, q_r) & \text{if } x > 0.
\end{cases}
$$

We denote by u the vector (ρ, q). We define u_m by the solution in Ω_c of the system

(4.2)
$$\begin{cases} \frac{q_m}{\rho_m} = \frac{q_l}{\rho_l}, \\ v_c(u_m) = v_c(u_r), \end{cases}$$

which yields a quadratic polynomial in ρ_m. We address the general case where the solution u_m of system (4.2) can coincide with u_l or u_r.

Case 1. $u_l \in \Omega_f$ and $u_r \in \Omega_f$. For all values of (ρ_l, ρ_r), the solution consists of a contact discontinuity from u_l to u_r.

Case 2. $u_l \in \Omega_c$ and $u_r \in \Omega_c$.

(i) If $q_l > 0$ and $v_c(u_r) \geq v_c(u_l)$, then the solution consists of a 1-rarefaction wave from u_l to u_m and a 2-contact discontinuity from u_m to u_r.

(ii) If $q_l > 0$ and $v_c(u_l) > v_c(u_r)$, then the solution consists of a shock wave from u_l to u_m and a 2-contact discontinuity from u_m to u_r.

(iii) If $q_l = 0$, then the solution consists of a 1-contact discontinuity from u_l to u_m and a 2-contact discontinuity from u_m to u_r.

(iv) If $0 > q_l$ and $v_c(u_r) > v_c(u_l)$, then the solution consists of a shock wave from u_l to u_m and a 2-contact discontinuity from u_m to u_r.

(v) If $0 > q_l$ and $v_c(u_l) \geq v_c(u_r)$, then the solution consists of a 1-rarefaction wave from u_l to u_m and a 2-contact discontinuity from u_m to u_r.

Case 3. $u_l \in \Omega_c$ and $u_r \in \Omega_f$.

(i) If $0 > q_l$, then the solution consists of a shock wave from u_l to u_m and a contact discontinuity from u_m to u_r.

(ii) If $q_l = 0$, then the solution consists of a 1-contact discontinuity from u_l to u_m and a contact discontinuity from u_m to u_r.

(iii) If $q_l > 0$, then the solution consists of a 1-rarefaction wave from u_l to u_m and a contact discontinuity from u_m to u_r.

Case 4. $u_l \in \Omega_f$ and $u_r \in \Omega_c$ Let u_{m-} be defined by the solution in Ω_c of the system

$$\begin{cases} \frac{q_{m-}}{\rho_{m-}} = \frac{q_-}{R}, \\ v_c(u_{m-}) = v_c(u_r), \end{cases}$$

and let $\Lambda(u_l, u_{m-})$ be the Rankine–Hugoniot phase transition speed between u_l and u_{m-} defined by (3.8).

(i) If $\Lambda(u_l, u_{m-}) \geq \lambda_1(u_{m-})$, then the solution consists of a phase transition from u_l to u_{m-} and a 2-contact discontinuity from u_{m-} to u_r.

(ii) If $\Lambda(u_l, u_{m-}) < \lambda_1(u_{m-})$, then let u_p be defined by the solution in Ω_c of the system

$$\begin{cases} \frac{q_p}{\rho_p} = \frac{q_-}{R}, \\ \Lambda(u_l, u_p) = \lambda_1(u_p). \end{cases}$$

The solution consists of a phase transition from u_l to u_p, a 1-rarefaction wave from u_p to u_{m-}, and a 2-contact discontinuity from u_{m-} to u_r.

4.3. Model properties. The properties of the Newell–Daganzo model can be abstracted from the definition of the Riemann solver in the previous section.

The nature of the Lax curves in congestion is identical to the original Colombo model and the Newell–Daganzo phase transition model (see Figure 3.3). Thus the solution for each model differs only when a free-flow state is involved. Three differences appear in that case:

(i) For a given density corresponding to the free-flow phase, the associated velocity differs in general between the two models.

(ii) Within the free-flow phase, only contact discontinuity can arise in the Newell–Daganzo phase transition model, whereas rarefaction waves and shockwaves can arise in the original Colombo model.

(iii) A transition from congestion to free-flow always involves a shock-like phase transition in the Colombo model (and thus the solution is composed of three waves in general), whereas the transition occurs through a metastable state in the Newell–Daganzo phase transition model, and involves only a "congestion to metastable" wave and a "metastable to free-flow" contact discontinuity.

These properties are illustrated in the next section on a Riemann problem.

As in the original Colombo phase transition model [8], the 1-Lax curves are LD for $q = 0$, and the direction of the rarefaction waves changes according to the sign of q. This yields interesting modeling capabilities, but requires the Riemann solver to be more complex than the one described in the following section.

Remark 4.2. As illustrated in Figure 3.2, the flux is linear in congestion at the standard state as per the Newell–Daganzo flux function. Remark 3.14 states that this shape models neutral drivers (aggressivity-wise). When the traffic is above the standard state (meaning that the velocity is higher than it is for the same density at the standard state), the 1-Lax curves are concave in $(\rho, \rho v)$ coordinates (meaning that the drivers are more aggressive). So, such a fundamental diagram shape seems to be in accordance with the intuition that, for a given density, the most aggressive drivers tend to have a greater speed. This is symmetrically true for less aggressive drivers, also accounted for by this model.

4.4. Benchmark test. In this section we compare the numerical solution given by the modified Godunov scheme with the analytical solution to a Riemann problem. We use the phase transition model (3.2) in the Newell–Daganzo case (4.1) with the following choice of parameters: $V = 45$, $R = 1000$, $\sigma_- = 190$, $\sigma = 220$, $\sigma_+ = 270$. The benchmark test is a phase transition from congestion to free-flow with the following left and right states.

(i) $u_l = (800, -0.1)$, which corresponds to congestion below standard state with $\rho = 800$ and $v = 2.9$.

(ii) $u_r = (100)$, which corresponds to a free-flow state with $\rho = 100$ and $v = 45$. This configuration gives rise to a shock wave between u_l and a congested state u_m followed by a contact discontinuity between u_m and u_r (Riemann case 3, first subcase), as shown in Figure 4.1.

We also present the solution given by the original Colombo model with the following parameters: $V_{c+} = 45$, $V_{f-} = 57$, $V = 67$, $q^* = 0$, $Q^- = -0.88$, and $Q^+ = 1.15$. The congested phases in the two models are identical with this choice of parameters. One may note that because the fundamental diagram in free-flow differs between the original Colombo model and the Newell–Daganzo phase transition model (see Figure 3.3), the speed corresponding to the right initial state in the Riemann problem is greater in the Colombo model.

The solutions to the Riemann problem for each model differ on several points. First, the intermediary state u_m belongs to the metastable phase in the Newell–Daganzo model, whereas it belongs to the free-flow phase for the Colombo model. Second, the wave from the intermediary state u_m to the right state u_r is a rarefaction wave in the Colombo model (as illustrated in Figure 4.1), whereas it is a contact discontinuity in the Newell–Daganzo phase transition model.
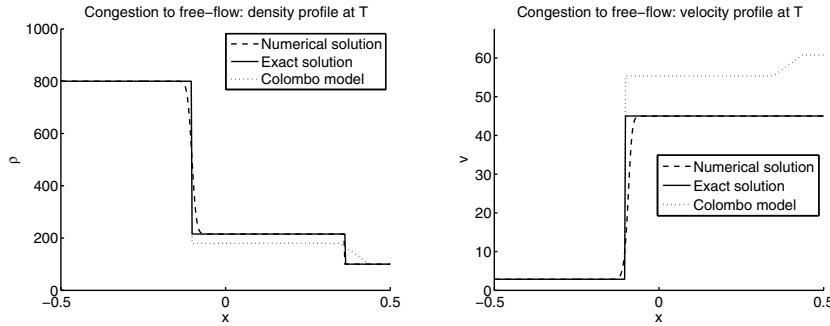
FIG. 4.1. *Exact solution (continuous line), computed solution (dashed line), and exact solution for the Colombo model (dotted line) for density (left) and speed (right). Between the two initial states, for the class of models presented in this article, a state $u_m = (215.4, -0.03)$ appears, which corresponds to the intersection of the* 1-*Lax curve going through u_l with the metastable phase. In this graph $T = 0.4$ and $\Delta x = 0.0013$.*

TABLE 4.1
Numerical error. Relative error between exact solution and the modified Godunov scheme solution for the benchmark described above, for different discretizations.

Cell $\sharp$	$E(T)$
50	$5.8 \ 10^{-04}$
100	$2.0 \ 10^{-04}$
200	$6.4 \ 10^{-05}$
400	$2.0 \ 10^{-05}$

The values of the error $E(T)$, as described in section 3.6 for $T = 4$ (a typical time for which all interactions have moved out of the computational domain) are outlined in Table 4.1.

5. The Greenshields phase transition model. In this section we use a Greenshields model to describe the velocity function in congestion, i.e., we use a concave quadratic flux function. We present the standard and perturbed flux functions, derive the corresponding Riemann solver which we test on a benchmark case, and describe the properties of the Greenshields phase transition model.

5.1. Analysis. We use a quadratic relation to describe the congestion standard state, which for physical considerations needs to satisfy the requirements from section 3.1. This leads us to choose the flux as a quadratic function of the form

$$\rho \, v_c^s(\rho) = (\rho - R)\,(a\,\rho + b)$$

such that the vanishing condition at $\rho = R$ is satisfied. Continuity at the critical density σ yields

$$b = \frac{\sigma\,V}{\sigma - R} - a\,\sigma,$$

so the flux at the standard state reads as

$$\rho \, v_c^s(\rho) = (\rho - R)\left(a\,(\rho - \sigma) + \frac{\sigma\,V}{\sigma - R}\right),$$

with a variation interval for a defined by the second and third conditions of section 3.1 as

$$a \in \left[-\frac{\sigma V}{(\sigma - R)^2}, 0 \right[.$$

Note that for the specific case in which $R = 2\sigma$ and a is defined by the fact that the derivative of the flux equals zero at σ (which reads as $a = -\sigma V/(\sigma - R)^2$), we obtain the classical Greenshields flux.

Following the general form given in system (3.3), we write the perturbed velocity function as

$$(5.1) \qquad \begin{cases} v_f(\rho) = V & \text{for } (\rho, q) \in \Omega_f, \\ v_c(\rho, q) = \left(1 - \frac{R}{\rho} \right) \left(a\,(\rho - \sigma) + \frac{\sigma V}{\sigma - R} \right)(1 + q) & \text{for } (\rho, q) \in \Omega_c, \end{cases}$$

with $a \in \left[-\frac{\sigma V}{(\sigma - R)^2}, 0 \right[$, and where Ω_f and Ω_c are defined by (3.4). The corresponding fundamental diagram is presented in Figure 5.1.
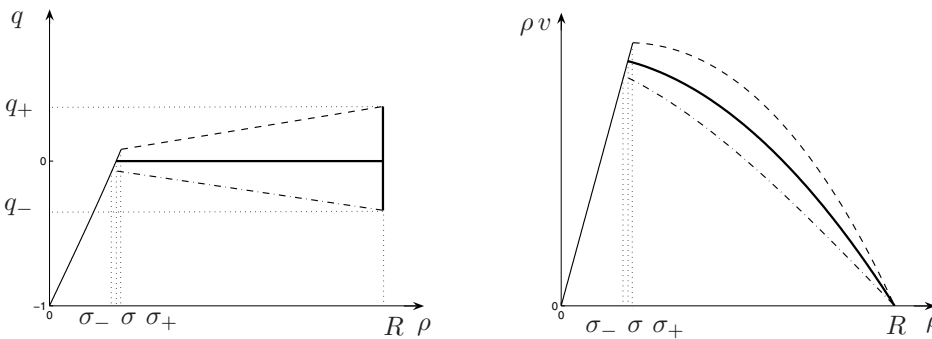

FIG. 5.1. *Phase transition model with a Greenshields standard state. Left: State space coordinates. Right: Flux-density coordinates. Thin solid line: Free-flow. Bold solid line: Congestion standard state. Thin dashed line: Upper bound of congestion. Thin dot-dashed line: Lower bound of congestion. The standard flux is concave, and all the 1-Lax curves are concave in $(\rho, \rho v)$ coordinates. In (ρ, q) coordinates the free-flow phase is not a straight line but has a very light convexity.*

Remark 5.1. The expression of the velocity function given by system (5.1) enables a set-valued velocity function for $\rho > \sigma_-$. For a given density the variable velocity can take several values. The lower bound of the congestion phase is concave, unlike for the model presented in section 4. This feature may be more appropriate for usual experimental datasets.

The requirements from section 3.2 here reduce to

$$q_- > -\frac{a\,R}{\frac{\sigma V}{\sigma - R} + a\,(2\,R - \sigma)}.$$

While for the Newell–Daganzo phase transition model the bound on the perturbation is given by the fact that the speed had to be positive, here the bound is given by the requirement on the constant concavity of the 1-Lax curves.

Remark 5.2. The lower bound on the perturbation is an increasing function of the parameter a, so this parameter should be chosen as small as possible to allow for more freedom, namely $a_{\min} = -\sigma V/(\sigma - R)^2$, which yields the lowest lower bound $q_-^{\min} = R/(2\,\sigma - 3\,R)$.

5.2. Solution to the Riemann problem. We consider the Riemann problem for system (3.2) with the velocity function from (5.1) and the initial datum

(5.2)
$$(\rho, q)(0, x) = \begin{cases} (\rho_l, q_l) & \text{if } x < 0, \\ (\rho_r, q_r) & \text{if } x > 0. \end{cases}$$

We follow the method used in [8] to construct the solution. We define u_m by the solution in Ω_c of the system

(5.3)
$$\begin{cases} \frac{q_m}{\rho_m} = \frac{q_l}{\rho_l}, \\ v_c(u_m) = v_c(u_r), \end{cases}$$

which yields a quadratic polynomial in ρ_m with one root in $[0, R]$. In the general case, the solution u_m of the system (5.3) can be equal to u_l or u_r.

Case 1. $u_l \in \Omega_f$ and $u_r \in \Omega_f$. For all values of (ρ_l, ρ_r) the solution consists of a contact discontinuity from u_l to u_r.

Case 2. $u_l \in \Omega_c$ and $u_r \in \Omega_c$.

(i) If $v_c(u_r) \geq v_c(u_l)$, then the solution consists of a 1-rarefaction wave from u_l to u_m and a 2-contact discontinuity from u_m to u_r.

(ii) If $v_c(u_l) > v_c(u_r)$, then the solution consists of a shock wave from u_l to u_m and a 2-contact discontinuity from u_m to u_r.

Case 3. $u_l \in \Omega_c$ and $u_r \in \Omega_f$. The solution consists of a 1-rarefaction wave from u_l to u_m and a contact discontinuity from u_m to u_r.

Case 4. $u_l \in \Omega_f$ and $u_r \in \Omega_c$. Let u_{m-} be defined by the solution in Ω_c of the system

$$\begin{cases} \frac{q_{m-}}{\rho_{m-}} = \frac{q_-}{R}, \\ v_c(u_{m-}) = v_c(u_r). \end{cases}$$

The solution consists of a phase transition from u_l to u_{m-} and a 2-contact discontinuity from u_{m-} to u_r.

Remark 5.3. The analysis in the case of a convex standard flux function, which we do not address in this article, is closely related to this case, modulo the sign of the parameter a and the concavity of the 1-Lax curves.

5.3. Model properties. The structure of the solution to the Riemann problem presented in the previous section explains the distinction with the original phase transition model.

(i) Since the 1-Lax curves are concave within the congestion phase, shock waves occur only from a low density on the left to a high density on the right. This is similar to classical traffic models with concave flux.

(ii) The concavity of the 1-Lax curves yields simple transitions from a free-flow state to a congested state. These phase transitions are composed of a shock-like phase transition followed by a contact discontinuity, whereas a rarefaction wave can appear between the two in the original phase transition model or in the Newell–Daganzo phase transition model.

(iii) Similarly to the Newell–Daganzo phase transition model, within the free-flow phase, the Greenshields phase transition model exhibits only contact discontinuities.

Another consequence of the fact that the 1-Lax curves are concave is that the Riemann solver is much simpler than in the Newell–Daganzo case, with only five

different types of solutions, compared to the Newell–Daganzo case which has eleven different types of solutions.

Remark 5.4. According to Remark 3.14, this flux function models aggressive drivers only, who drive along concave 1-Lax curves. In practice, it is able to model a class of clouds of points observed experimentally, where the congested domain has a concave lower border in $(\rho, \rho v)$ coordinates.

5.4. Benchmark test. In this section we compare the numerical results given by the modified Godunov scheme on a benchmark test with its analytical solution. We use the phase transition model (3.2) in the Greenshields case (5.1) with the following choice of parameters: $V = 45$, $R = 1000$, $\sigma_- = 190$, $\sigma = 200$, and $\sigma_+ = 215$. We choose $a = -0.01$. The resulting values for the extrema of the perturbation are $q_- = -0.34$ and $q_+ = 0.44$. The benchmark test is a phase transition from free-flow to congestion, with the following left and right states.

(i) $u_l = (180)$, which corresponds to a free-flow state with $\rho = 180$ and $v = 45$.

(ii) $u_r = (900, 0.2)$, which corresponds to a congested situation above standard state with $\rho = 900$ and $v = 2.4$.

This configuration gives rise to a phase transition between u_l and a congested state u_m followed by a 2-contact discontinuity between u_m and u_r (Riemann case 4), which is illustrated in Figure 5.2.

We also present the solution to the Riemann problem for the original Colombo model with parameters $V_{c+} = 45$, $V_{f-} = 57$, $V = 67$, $q^* = 0$, $Q^- = -0.32$, and $Q^+ = 0.44$. The speed in free-flow differs between the two models. The phase transition speed is negative for both models but is greater in the case of the Greenshields phase transition model, which models more aggressive drivers which have a higher flux in congestion for the same density value. The second wave has the same speed in the two models.

Table 5.1 summarizes the values of the error $E(T)$, as defined in section 3.6, for different sizes of the discretization step, at $T = 4$.
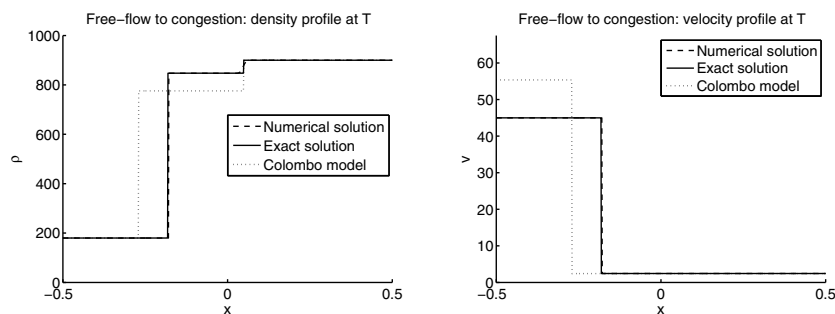

FIG. 5.2. *Exact solution (continuous line), computed solution (dashed line), and solution to the Colombo model (dotted line) for density (left) and speed (right). Between the two initial states a state $u_m = (847.4, -0.24)$ appears, which corresponds to the intersection of the lower bound of the diagram in congestion with the 2-Lax curve going through u_r. In this graph $T = 1$ and $\Delta x = 0.0013$.*

TABLE 5.1
Relative error between exact solution and numerical solution for the test case explicitly described previously, for different numbers of space cells.

Cell ♯	$E(T)$
50	$3.1 \ 10^{-04}$
100	$7.8 \ 10^{-05}$
200	$2.1 \ 10^{-05}$
400	$5.4 \ 10^{-06}$

6. Conclusion. This article reviewed the fundamental features of the Colombo phase transition model and proposed building a class of models upon it in which the fundamental diagram is set-valued in the congested regime. The notion of standard state, which provides the basis for the construction of the 2×2 phase transition models, was introduced. General conditions which enable the extension of the original Colombo phase transition model to this new class of 2×2 phase transition models were investigated. A modified Godunov scheme which can be applied to models with nonconvex state space was used to solve these equations numerically. The model was instantiated for two specific flux functions, which include the Newell–Daganzo flux function (affine) and the Greenshields flux function (quadratic concave). A discussion of the choice of parameters needed for each of the models was conducted. The solution to the Riemann problem was derived, and a validation of the numerical results using benchmark tests was conducted. Open questions for this model include the capability of the model to accurately reproduce traffic features experimentally measured on highways. Experimental validations of the model should reveal its capabilities of reproducing traffic flow more accurately than existing models. In addition, the specific potential of the model to integrate velocity measurements (through proper treatment of the second state variable of the problem) is a significant advantage of this model over any first order model for which the density-flux relation is single valued. The proper use of this key feature for data assimilation is also an open problem, which could have very promising outcomes for highway traffic state estimation.

REFERENCES

[1] A. AW AND M. RASCLE, *Resurrection of "second order" models of traffic flow*, SIAM J. Appl. Math., 60 (2000), pp. 916–938.
[2] C. BARDOS, A.-Y. LE ROUX, AND J.-C. NÉDÉLEC, *First order quasilinear equations with boundary conditions*, Comm. Partial Differential Equations, 4 (1979), pp. 1017–1034.
[3] S. BLANDIN, G. BRETTI, A. CUTOLO, AND B. PICCOLI, *Numerical simulations of traffic data via fluid dynamic approach*, Appl. Math. Comput., 210 (2009), pp. 441–454.
[4] A. BRESSAN, *Hyperbolic Systems of Conservation Laws: The One-Dimensional Cauchy Problem*, Oxford Lecture Ser. Math. Appl. 20, Oxford University Press, Oxford, UK, 2000.
[5] M. CASSIDY AND J. WINDOVER, *Methodology for assessing dynamics of freeway traffic flow*, Transportation Research Record, 1484 (1995), pp. 73–79.
[6] C. CHALONS AND P. GOATIN, *Godunov scheme and sampling technique for computing phase transitions in traffic flow modeling*, Interfaces Free Bound., 10 (2008), pp. 195–219.
[7] R. COLOMBO, *On a 2×2 hyperbolic traffic flow model*, Math. Comput. Modelling, 35 (2002), pp. 683–688.
[8] R. M. COLOMBO, *Hyperbolic phase transitions in traffic flow*, SIAM J. Appl. Math., 63 (2002), pp. 708–721.
[9] R. COLOMBO, P. GOATIN, AND F. PRIULI, *Global well-posedness of traffic flow models with phase transitions*, Nonlinear Anal., 66 (2007), pp. 2413–2426.
[10] C. DAGANZO, *The cell transmission model: A dynamic representation of highway traffic consistent with the hydrodynamic theory*, Transportation Res. Part B, 28 (1994), pp. 269–287.

[11] C. Daganzo, *The cell transmission model, Part* II: *Network traffic*, Transportation Res. Part B, 29 (1995), pp. 79–93.

[12] C. Daganzo, *Requiem for second-order fluid approximations of traffic flow*, Transportation Res. Part B, 29 (1995), pp. 277–286.

[13] C. Daganzo, M. Cassidy, and R. Bertini, *Possible explanations of phase transitions in highway traffic*, Transportation Res. Part A, 33 (1999), pp. 365–379.

[14] J. Del Castillo and F. Benitez, *On the functional form of the speed-density relationship* I: *General theory*, Transportation Res. Part B, 29 (1995), pp. 373–389.

[15] J. Del Castillo, P. Pintado, and F. Benitez, *The reaction time of drivers and the stability of traffic flow*, Transportation Res. Part B, 28 (1994), pp. 35–60.

[16] M. Garavello and B. Piccoli, *Traffic Flow on Networks*, AIMS Ser. Appl. Math. 1, AMS, Springfield, MO, 2006.

[17] M. Garavello and B. Piccoli, *On fluido-dynamic models for urban traffic*, Netw. Heterog. Media, 4 (2009), pp. 107–126.

[18] J. Glimm, *Solutions in the large for nonlinear hyperbolic systems of equations*, Comm. Pure Appl. Math., 18 (1965), pp. 697–715.

[19] P. Goatin, *The Aw-Rascle vehicular traffic flow model with phase transitions*, Math. Comput. Modelling, 44 (2006), pp. 287–303.

[20] S. Godunov, *A difference method for numerical calculation of discontinuous solutions of the equations of hydrodynamics*, Sb. Math., 89 (1959), pp. 271–306.

[21] H. Greenberg, *An analysis of traffic flow*, Oper. Res., 7 (1959), pp. 79–85.

[22] B. Greenshields, *A study of traffic capacity*, Proceedings of the Highway Research Board, 14 (1935), pp. 448–477.

[23] H. Holden and N. Risebro, *Front Tracking for Hyperbolic Conservation Laws*, Appl. Math. Sci. 152, Springer-Verlag, New York, 2002.

[24] Z. Jia, C. Chen, B. Coifman, and P. Varaiya, *The PeMS algorithms for accurate, real-time estimates of g-factors and speeds from single-loop detectors*, in Intelligent Transportation Systems, 2001, pp. 536–541.

[25] B. Kerner, *Experimental features of self-organization in traffic flow*, Phys. Rev. Lett., 81 (1998), pp. 3797–3800.

[26] B. Kerner, *Phase transitions in traffic flow*, Traffic and Granular Flow, (2000), pp. 253–283.

[27] S. Kruzhkov, *First order quasilinear equations in several space variables*, Sb. Math., 10 (1970), pp. 217–243.

[28] J. Lebacque, *The Godunov scheme and what it means for first order macroscopic traffic flow models*, in Proceedings of the 13th ISTTT, Lyon, France, 1996, pp. 647–677.

[29] P. Le Floch, *Explicit formula for scalar non-linear conservation laws with boundary conditions*, Math. Methods Appl. Sci., 10 (1988), pp. 265–287.

[30] R. J. LeVeque, *Finite Volume Methods for Hyperbolic Problems*, Cambridge Texts Appl. Math., Cambridge University Press, Cambridge, UK, 2002.

[31] M. Lighthill and G. Whitham, *On kinematic waves* II: *A theory of traffic flow on long crowded roads*, Proc. R. Soc. Lond. Ser. A Math. Phys. Eng. Sci., 229 (1956), pp. 317–345.

[32] W. Lin and D. Ahanotu, *Validating the Basic Cell Transmission Model on a Single Freeway Link*, Technical report, Institute of Transportation Studies, University of California, Berkeley, 1995.

[33] L. Munoz, X. Sun, R. Horowitz, and L. Alvarez, *Traffic density estimation with the cell transmission model*, in Proceedings of the 2003 American Control Conference, Vol. 5, 2003, pp. 3750–3755.

[34] G. Newell, *A simplified theory of kinematic waves in highway traffic* II: *Queueing at freeway bottlenecks*, Transportation Res. Part B, 27 (1993), pp. 289–303.

[35] O. Oleinik, *Discontinuous solutions of non-linear differential equations*, Uspekhi Mat. Nauk, 12 (1957), pp. 3–73.

[36] M. Papageorgiou, *Some remarks on macroscopic traffic flow modelling*, Transportation Res. Part A, 32 (1998), pp. 323–329.

[37] H. Payne, *Models of freeway traffic and control*, Math. Models Public Syst., 1 (1971), pp. 51–61.

[38] P. Richards, *Shock waves on the highway*, Oper. Res., 4 (1956), pp. 42–51.

[39] D. Serre, *Systems of Conservation Laws*, Diderot, Paris, 1996.

[40] I. Strub and A. Bayen, *Weak formulation of boundary conditions for scalar conservation laws: An application to highway traffic modelling*, Internat. J. Robust Nonlinear Control, 16 (2006), pp. 733–748.

[41] B. Temple, *Systems of conversation laws with invariant submanifolds*, Trans. Amer. Math. Soc., 280 (1983), pp. 781–795.

[42] L. Tong, *Nonlinear dynamics of traffic jams*, Phys. D, 207 (2005), pp. 41–51.

[43] E. Toro, *Riemann Solvers and Numerical Methods for Fluid Dynamics*, Springer-Verlag, Berlin, 1997.

[44] R. Underwood, *Speed, volume, and density relationships: Quality and theory of traffic flow*, Yale Bureau of Highway Traffic, (1961), pp. 141–188.

[45] P. Varaiya, *Reducing highway congestion: An empirical approach*, Eur. J. Control, 11 (2005), pp. 301–309.

[46] P. Varaiya, *Congestion, ramp metering and tolls*, Philos. Trans. R. Soc. Lond. Ser. A Math. Phys. Eng. Sci., 366 (2008), pp. 1921–1930.

[47] Y. Wang and M. Papageorgiou, *Real-time freeway traffic state estimation based on extended Kalman filter: A general approach*, Transportation Res. Part B, 39 (2005), pp. 141–167.

[48] G. Whitham, *Linear and Nonlinear Waves*, Pure Appl. Math., Wiley Interscience, New York, 1974.

[49] H. Zhang, *A theory of nonequilibrium traffic flow*, Transportation Res. Part B, 32 (1998), pp. 485–498.

[50] H. Zhang, *A non-equilibrium traffic model devoid of gas-like behavior*, Transportation Res. Part B, 36 (2002), pp. 275–290.